Evaluation and Optimization of The Bit Rate - Distance Relationships in IR-UWBoF Systems

Mohamed Shehata[1], Mohamed Sameh Said[1], and Hassan Mostafa[1,2]
[1]Electronics and Communication Engineering Department, Cairo University, Giza 12613, Egypt.
[2]Nanotechnology and Nanoelectronics Program, Zewail City for Science and Technology, Giza 12588, Egypt

***Abstract*—In this paper, the achievable bit rate as well as the maximum wireless reach of Gaussian and sech-based impulse radio ultrawide band (IR-UWB) signals are investigated. A typical UWB-over-fiber (UWBoF) system incorporating photonic generation and wireless transmission of these waveform types is considered and the performances of both waveform types are compared, with the bit rate - wireless transmission distance as the performance metric of interest. Transmission distances are maximized at the forward error correction (FEC) bit error rate limit under the severe spectral constrains of the Federal Communications Committee (FCC).**

***Index Terms*—Impulse radio (IR), microwave photonic (MWP), ultra wideband over fiber (UWBoF).**

I. Introduction

The extremely low spectral bounds regulated by the FCC on the spectra of UWB signals [1] restricts the maximum wireless reach of these signals to only 4-10 m. Moreover, the wireless propagation of UWB signals is susceptible to the frequency-selective path loss offered by the UWB channels. This loss tends to further decrease the UWB signal power below the sensitivity threshold of a UWB receiver and might prevent remotely located users from the high speed wireless services offered by UWB systems. Microwave photonic (MWP) techniques have been employed to produce UWB signals in the optical domain and to enable the distribution of the photonically generated waveforms over low loss optical fiber links to the geographically remote users at their locations. At these remote locations, UWB signals are transformed back to the electrical domain and are wirelessly re-distributed to the terminal users. Several approaches have been proposed to demonstrate the efficiency of integrating radio frequency (RF) and optical technologies, resulting in the development of UWB over fiber (UWBoF) systems with combined optical and wireless transmission. For instance, in [2], a 500 Mbps train of impulse radio UWB (IR-UWB) waveforms has been successfully generated and distributed in the optical domain before wireless transmission over a distance of 65 cm. In [3], a 30 cm UWB wireless transmission link has been utilized to transmit IR-UWB waveforms at a rate of 1.25 Gbps. A higher transmission rate of 1.625 Gbps at a wireless transmission distance as short as 20 cm has been reported in [4]. Furthermore, in [5], the wireless transmission of a 1.6875 Gbps stream of IR-UWB waveforms has been enabled by a 5 cm wireless link. In [6], the wireless distribution of a 3.125 Gbps train of IR-UWB waveforms has been recorded at the expense of the wireless range between a TX-RX antenna pair. This same rate has been also observed in [7] over a wireless transmission range of 2.9 m. It should be highlighted that, in [7], the emission levels of the transmitted IR-UWB waveforms has been increased by 10 dBm above the admissible FCC spectral limits. Interestingly, the reported experimental results confirm the inevitable decrease of the wireless transmission distance at the expense of increasing the signalling bit rate in IR-UWBoF systems. However, to the best of the authors' knowledge, no study has been reported to quantify this inverse relationship. In this work, the upper bounds of the bit rate - wireless transmission distance relationships in IR-UWBoF systems are numerically evaluated and are optimized, considering the impact of the UWB channel frequency response on IR-UWB waveforms derived from Gaussian-based and sech pulses. The rest of this paper is structured as follows. A typical IR-UWBoF communication system with combined optical and wireless transmission chains is overviewed in Section II. Also in Section II, the bit rate - distance relationships are developed in terms of the IR-UWB signal spectra and the channel model. These expressions are then numerically evaluated and analyzed in Section III. Based on the obtained results, a conclusion is drawn and is finally presented in Section IV.

II. System Model Overview

Fig.1 depicts a typical block diagram for the photonic generation, transmission and wireless distribution processes in a typical IR-UWBoF system. As clear from this figure, the system consists of an MWP filter coupled to an electrical UWB transmitter, which exists in a central office (CO), via an optical fiber transmission link, a wireless UWB channel and a UE, where the UWB receiver exists. The input to the MWP processing stage is a sequence of independent and identically distributed (i.i.d) binary data symbols. In addition to the photonic generation of IR-UWB waveforms, the MWP processing filter encodes each information symbol by the produced waveform, which is propagated down an optical fiber link to the CO at which the photodetection process is applied.

At the CO, the photodetected waveform is proportional to the m^{th} order derivative of a basis function $\psi(t,\tau)$, where τ is its full width at half maximum pulse width. This basis function is an amplitude normalized Gaussian pulse, typically expressed as $\psi(t,\tau) = \exp(-t^2/{\tau_g}^2)$, or an amplitude normalized sech pulse, expressed as $\psi(t,\tau) = sech(t/\tau)$. The FWHM pulse width τ of the input basis function is related to the Gaussian pulse width as $\tau_g \triangleq \tau/2\sqrt{\log(2)}$, whereas for the sech pulse

978-1-5386-7392-8/18/$31.00 ©2018 IEEE

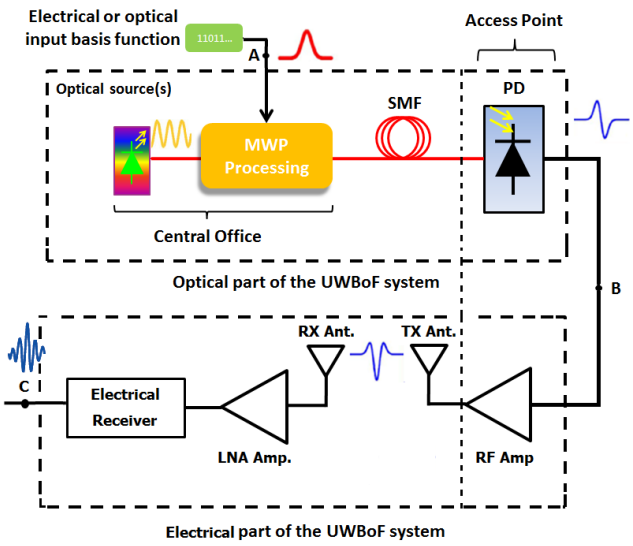

Fig. 1. Typical block diagram of an IR-UWBoF system with combined optical and wireless transmission. MWP: microwave photonic, SMF: single mode fiber, PD: photodetector, RF: radio frequency, Amp: amplifier, and LNA: low noise amplifier. Red lines: optical signal routes. Black lines: electrical signal routes.

is related to τ as $\tau_s \triangleq \tau/2sech^{-1}(0.5)$. In this context, it is assumed that the RF waveform at the TX antenna is related to $\psi(t,\tau)$ as $\psi^{(m)}(t,\tau) = \sqrt{E_{b,m}}d^m\psi(t,\tau)/dt^m; (t,\tau) \in \mathbf{R}$, where $E_{b,m}$ is energy of a bit encoded by the waveform $\psi^{(m)}(t,\tau)$. It is important to note that $E_{b,m}$ scales the power spectral density (PSD) of a IR-UWB signal to the maximum PSD admissible by the FCC mask within the useful UWB band, bounded by a lower and a higher cutoff frequencies of f_L and f_H, respectively. Mathematically, $E_{b,m}$ is given by

$$E_{b,m} \triangleq \max\{S_{FCC}(\omega)\} / \max\left\{\left|\Psi^{(m)}(j\omega,\tau)\right|^2\right\} \quad (1)$$

where $S_{FCC}(\omega)$ is the FCC spectral, $\omega = 2\pi f$ is the angular frequency, $\Psi^{(m)}(j\omega,\tau) = \Im\{d^m\psi(t,\tau)/dt^m\}$ and $\Im\{.\}$ designates the Fourier transform operator. The Fourrier transform of an m^{th} order Gaussian-based derivative, normalized to FCC spectral mask, is given by

$$\Psi^{(m)}_{n,FCC}(j\omega,\tau_g) = \sqrt{E_{g,m}}(j\omega)^m\tau_g\sqrt{\pi}\exp(-(\omega\tau_g)^2/2) \quad (2)$$

where $E_{g,m}$ is the energy of a bit encoded by an m^{th} order Gaussian-based IR-UWB waveform, while the FCC normalized Fourrier transform of the m^{th} order sech-based derivative is given by

$$\Psi^{(m)}_{n,FCC}(j\omega,\tau_s) = \sqrt{E_{s,m}}(j\omega)^m 4\pi\tau_s\text{sech}(2\pi\omega\tau_s) \quad (3)$$

where $E_{s,m}$ is the energy of a bit encoded by an m^{th} order sech-based IR-UWB waveform. The electrical RF spectra of Gaussian and sech-based IR-UWB waveforms along with the FCC spectral constraints are shown in Figs. 2 (a) and (b), respectively. In this context, $\Psi^{(m)}_{n,FCC}(\omega,\tau)$ refers to one of the definitions in (2) or (3) as required. Substituting each of the definitions in $\partial\left|\Psi^{(m)}_{n,FCC}(\omega,\tau)\right|^2/\partial\omega = 0$ and solving for

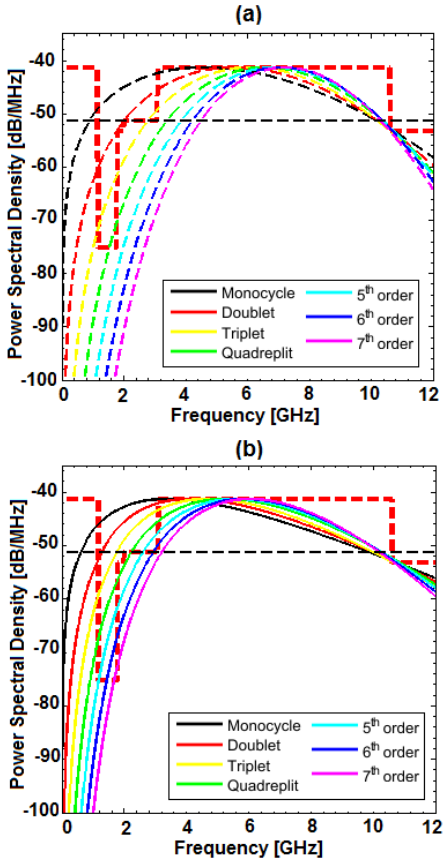

Fig. 2. Simulated electrical RF spectra of (a): Gaussian-based IR-UWB waveforms and (b): sech-based IR-UWB waveforms. Red dashed line: the FCC spectral mask. Black dashed line: the -51.3 dBm/MHz power spectral density limit to determine the -10 dB bandwidth.

ω yields the peak emission angular frequencies $\omega_{p,g}$ and $\omega_{p,s}$, defined as the angular frequencies at which $\left|\Psi^{(m)}(j\omega,\tau)\right|^2 = \max\left\{\left|\Psi^{(m)}(j\omega,\tau)\right|^2\right\}$ for Gaussian and sech-based IR-UWB waveforms, respectively. The corresponding bit energies $E_{g,m}$ and $E_{s,m}$ are obtained by

$$E_{g,m} = S_{FCC}(\omega)\exp\left((\omega_{p,g}\tau_g)^2/2\right)/\omega^{2m}_{p,g}\pi\tau_g^2 \quad (4)$$

$$E_{s,m} = S_{FCC}(\omega)\cosh^2(2\pi\omega_{p,s}\tau_s)/\omega^{2m}_{p,s}(4\pi\tau_s)^2 \quad (5)$$

Nevertheless, both the optical fiber and the wireless transmission chains influence the spectra of the IR-UWB waveform after the photonic generation and photodetection processes, respectively. However, throughout the analysis it is assumed that the RF amplifier at the access point compensates for the loss in the IR-UWB signal power due to the optical fiber transmission and the optical-to-electrical conversion efficiency. Moreover, the length of the optical fiber link is assumed to be sufficiently small, such that chromatic dispersion effects are negligible and the pulse width of the photonically generated IR-UWB is essentially invariant with the optical fiber length. Moreover, it is assumed that the IR-UWB waveforms are transmitted over a typical path loss channel with an arbitrary path loss exponent γ. In this context, the squared magnitude

frequency response of this channel model $PL(\omega)$ is expressed as [8]

$$PL(\omega) = \frac{G_{TX}(\omega)G_{RX}(\omega)c^2}{4\omega^2 D^\gamma} \tag{6}$$

where $G_{TX}(\omega)$ and $G_{RX}(\omega)$ are the frequency responses of the UWB transmit and receive antennas respectively, c is the speed of light and D is the wireless transmission distance between the transmit and receive antennas. There exists a general relationship between the wireless transmission reach and the transmission bit rate. This relationship is expressed, as a function of the channel frequency response as well as the UWB signal spectrum, as [9]:

$$D = \left(\frac{1}{2\pi \left(\frac{E_b}{N_o}\right) R_b k_B T_o.NF.LM} \int_{\omega_L}^{\omega_H} PL(\omega)\Phi(\omega)d\omega \right)^{1/\gamma} \tag{7}$$

where E_b/N_o is the bit energy to noise PSD ratio, R_b is the bit rate of the UWB wireless transmission link, k_B is the Boltzmann constant and T_o is the nominal receiver noise temperature, *NF* is the noise figure, *LM* is the link margin, $\omega_H = 2\pi f_H, \omega_L = 2\pi f_L$ and $\Phi(\omega)$ is the PSD of the transmitted IR-UWB waveform, normalized to the maximum admissible FCC PSD. It should be noted that, the spectral and the spatial characteristics of the TX and the RX antennas depend on the particular design of each antenna. For simplicity, each of the two antennas is assumed to have a quasi-flat frequency response within the useful UWB band and is aligned along the direction of its maximum radiation. Accordingly, $G_{TX}(\omega)$ and $G_{RX}(\omega)$ are replaced by equivalent constant gains of G_{TX} and G_{RX}, respectively. Moreover, the value of E_b/N_o depends on the particular modulation scheme and is given by the inverse bit error rate (BER) function of this scheme such that the BER does not exceed the forward error correction (FEC) limit value of 10^{-3}. Substituting (6) in (7), the bit rate - distance relationship can be re-stated as follows:

$$D = \lambda R_b^{-1/\gamma} \tag{8}$$

where λ is a proportionality constant that is given by

$$\lambda \triangleq \left(\frac{G_{TX}G_{RX}c^2}{8\pi \left(\frac{E_b}{N_o}\right) k_B T_o.NF.LM} \int_{\omega_L}^{\omega_H} \omega^{-2}\Phi(\omega)d\omega \right)^{1/\gamma} \tag{9}$$

Obviously, λ includes the design parameters of the IR-UWBoF wireless transmission chain as well as the parameters of the IR-UWB signalling waveform. For Gaussian-based IR-UWB waveforms, λ is denoted by $\lambda_{g,m}$ and is given, in terms of (2) and (9), by

$$\lambda_{g,m} \triangleq \left(\frac{(c\tau_g)^2 G_{TX}G_{RX}E_{g,m}}{8 \left(\frac{E_b}{N_o}\right) k_B T_o.NF.LM} \int_{\omega_L}^{\omega_H} \omega^\mu \exp\left(-(\omega\tau_g)^2\right) d\omega \right)^{1/\gamma} \tag{10}$$

where $\mu = 2m - 2$. Similarly, for sech-based IR-UWB waveforms, the value of λ is denoted by $\lambda_{s,m}$ and is given by substituting (3) in (9) as follows:

$$\lambda_{s,m} = \left(\frac{2\pi(c\tau_s)^2 G_{TX}G_{RX}E_{s,m}}{\left(\frac{E_b}{N_o}\right) k_B T_o.NF.LM} \int_{\omega_L}^{\omega_H} \omega^\mu \mathrm{sech}^2\left(2\pi\omega\tau_s\right) d\omega \right)^{1/\gamma} \tag{11}$$

The upper bounds of the bit rate - distance relationship in (8) are obtained for Gaussian and sech-based IR-UWB waveforms by maximizing (10) and (11) with respect to τ_g and τ_s, respectively.

III. Simlation Results and Analysis

The integrals in (10) and (11) are evaluated using numerical integration techniques, considering the typical values for the IR-UWBoF system parameters, listed in Table I. The optimal pulse widths that maximize these integrals are obtained by numerically solving $\partial\lambda_{g,m}/\tau_g = 0$ and $\partial\lambda_{s,m}/\tau_s = 0$ for $\tau_g \in \mathbf{R}^+$ and $\tau_s \in \mathbf{R}^+$, respectively.

TABLE I
Simulation parameters

Parameter Name and Symbol	Value and Unit
UWB channel path loss exponent,γ	3.5
Lower UWB band cutoff frequency, f_L	3.1 GHz
Higher UWB band cutoff frequency, f_H	10.6 GHz
Maximum FCC PSD limit, $\max\{S_{FCC}(\omega)\}$	-41.3 dBm/MHz
Boltzmann constant, k_B	1.23×10^{-38} J/K
Nominal receiver noise temperature, T_o	300 K
Link margin, *LM*	0 dB
Link Noise figure, *NF*	0 dB
Signal-to-Noise ratio per bit, E_b/N_o	10 dB
FEC BER limit	10^{-3}
TX antenna gain, $G_{TX}(\omega)$	1
RX antenna gain, $G_{RX}(\omega)$	1
Pulse order, *m*	$\{1, 2, ...7\}$

Table (II) lists the optimal FWHM pulse widths that lead to maximizing (10) and (11), considering the first seven derivatives of the Gaussian and sech-based IR-UWB waveforms.

Figs. 3 (a) and (b) plot the wireless transmission distance versus the transmission bit rate with IR-UWB signalling using Gaussian and sech basis functions, respectively at different values of *m*. Clearly, both figures confirm the inverse relationship between the bit rate and the wireless transmission diatnce for both waveform types. In general, it is observed that, at the fixed bit rate, the maximum wireless transmission distance achieved by sech-based IR-UWB waveforms outperforms their corresponding Gaussian-based counterparts. For instance, the wireless reach of a Gaussian monocycle pulse at a signalling bit rate of 1 Gbps is about 4 m, while the sech monocycle pulse exceeds this reach by about 1 m. This is attributed to the rich spectral content in sech-based waveforms, compared to their Gaussian-based counterparts as clear from Figs. 2 (a) and (b). Moreover, for both waveform types, the transmission distance that can be achieved by a low order pulse is always higher than that can achieved by a pulse having a higher

TABLE II
OPTIMAL PULSE WIDTHS THAT MAXIMIZE (10) AND (11)

Pulse order, m	Monocycle	Doublet	Triplet	Quadruplet	5^{th} order	6^{th} order	7^{th} order
Gaussian-based	68.16 ps	104.2 ps	136.2 ps	164.2 ps	188.3 ps	212.3 ps	233.9 ps
Sech-based	15.13 ps	27.15 ps	41.17 ps	55.2 ps	71.23 ps	86.26 ps	103.3 ps

derivative order. The obtained results are consistent with the results obtained in [10]-[13] for the same waveform types and derivative orders, considering the power, the signal to noise ratio (SNR), the maximum wireless reach and the spectral radiation efficiency as the performance evaluation metrics of interest. These observations recommend Gaussian and sech monocycle pulses as candidate chip waveforms for power economic-high speed optical network on chip systems that are based on ultrashort optical orthogonal codes [14].

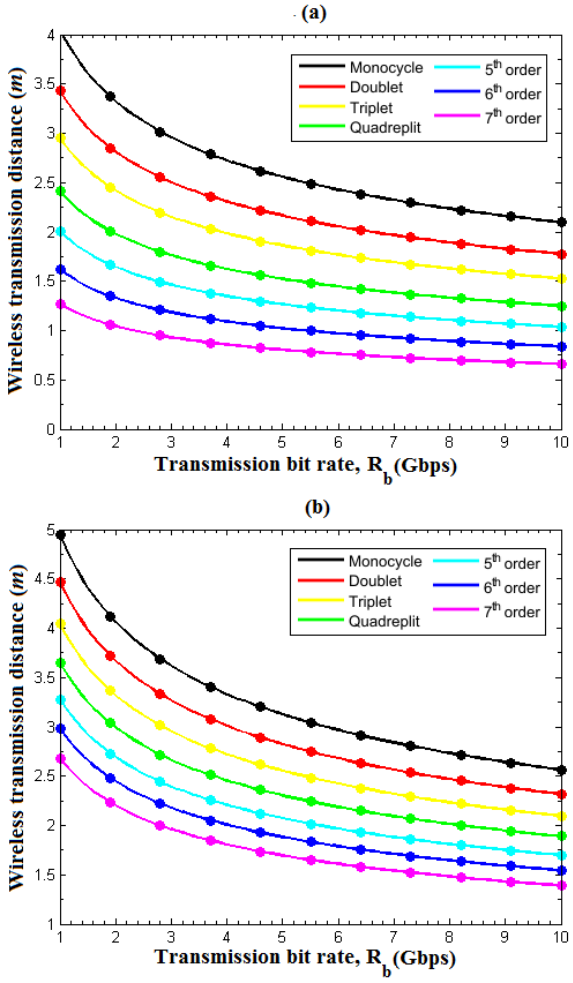

Fig. 3. Wireless transmission distance vs. the transmission bit rate with IR-UWB signalling using (a): Gaussian-input basis function and (b): sech input basis function at different values of m

IV. CONCLUSION

In this work, the bit rate - distance relationships in the wireless transmission chain of IR-UWBoF systems are evaluated, considering the impact of the UWB channel frequency response on the spectra of Gaussian-based and sech-based IR-UWB waveforms. Simulations results show that, the maximum wireless reach of the considered IR-UWB waveforms is strongly influenced by the waveform type and its temporal pulse widths.

ACKNOWLEDGMENT

This work was funded by telecommunications regulatory agency of Egypt (NTRA-Egypt).

REFERENCES

[1] US. Fed. Comm. Commission, First report and order, (Revision of part 15 of the commission's rules regarding ultra-wideband transmission systems), adopted February 14, 2002, released April 22, 2002. Tech. Rep.
[2] M. Abtahi, M. Mirshafiei, S. LaRochelle, and L. A. Rusch,"All-Optical 500 Mb/s UWB Transceiver: An Experimental Demonstration," *J. Lightwave Technol.*, vol. 26, no. 15, pp. 2795-2802, Aug. 2008.
[3] Y. M. Chang, J. Lee, D. Koh, H. Chung, and J. H. Lee, "Ultrawideband doublet pulse generation based on a semiconductor electroabsorption modulator and its distribution over a fiber/wireless link," *J. Opt. Commun. Netw.*, vol. 2, no. 8, pp. 600-608, Aug. 2010.
[4] H. Shams, A. Kaszubowska-Anandarajah, P. Perry, L. P. Barry, "Optical generation, fiber distribution and air transmission for ultra wide band over fiber system," in Optical Fiber Communication Conference and Exposition (OFC), Paper OWR, Mar. 2009.
[5] S. Pan and J. Yao, "Photonic generation of chirp-free UWB signals for UWB over fiber applications," in IEEE International Topical Meeting on Microwave Photonics (MWP), pp. 1-4, Oct. 2009.
[6] E. Zhou, X. Xu, K. Lui, and K. K. Wong, "High-speed photonic power-efficient ultra- wideband transceiver based on multiple PM-IM conversions," *IEEE Trans. Microw. Theory Tech.*, vol. 58, no. 11, pp. 3344-3351, Nov. 2010.
[7] T. B. Gibbon, X. Yu; R. Gamatham, N. Guerrero Gonzalez, R. Rodes, J. B. Jensen, A. Caballero, I. T. Monroy, "3.125 Gb/s impulse radio ultra-wideband photonic generation and distribution over a 50 km fiber with wireless transmission," *IEEE Microw. Wireless Compon. Lett.*, vol. 20, no. 2, pp. 127-129, Feb. 2010.
[8] T. Wang, W. Heinzelman and A. Seyedi ,"Link Energy Minimization in IR-UWB Based Wireless Networks," *IEEE Trans. Wireless Commun.*, vol. 9, no. 9, pp. 2800-2811, September, 2010.
[9] M. Ghavami, L. B. Michal and P. W. Daly,"Ultra Wide Band Signals and Systems in Communication Engineering," 2-nd ed. West Sussex, England: Wily, 2007.
[10] M. Shehata, H. Mostafa, and Y. Ismail, "On The Theoretical Limits of The Power EfiňAciency of Photonically Generated IR-UWB Waveforms", IEEE Journal of Lightwave Technology (JLT), vol. 36, issue 10, pp. 2017 - 2023, 2018.
[11] M. Shehata, H. Mostafa, and Y. Ismail, "Accurate Closed Form Expressions for The Bit Rate-Distance Relationship in IR-UWBoF Systems", IEEE Communications Letters, vol. 21, issue 10, pp. 2138-2141, 2017.
[12] M. Shehata, and H. Mostafa, "Photodetected Power Maximization of Photonically Generated Impulse Radio Ultrawide Band Signals", IEEE International Symposium on Circuits and Systems (ISCAS 2018), Florence, Italy, pp. 1-4, 2018.
[13] M. Shehata, H. Mostafa, and Y. Ismail, "Closed Form Expressions and Bounds for The Signal to Noise Ratio in IR-UWBoF Systems", IEEE Photonics Technology Letters, vol. 29, issue 6, pp. 507-510, 2017.
[14] Shehata, M., and Mostafa, H. âĂIJ A Single Wavelength Photonic Network on Chip Design Based on Optical Orthogonal Codes,âĂİ The 50-th IEEE International Symposium on Circuits & Systems (ISCAS.2018), Florence, Italy, May 2018.